Supplementary Information for

Ratiometric radio-photoluminescence dosimeter based on a radical excimer for X-Ray detection

Huangjie Lu[b,c] *, Jingqi Ma*[b,c]*, Junpu Yang*[a]*, Huiliang Hou*[b,c]*, Jiacheng Lu,*[a] *Jian-Qiang Wang*[b,*]*, Yaxing Wang,*[d] *Jian Lin*[a,*]

[a] School of Nuclear Science and Technology, Xi'an Jiaotong University, No.28, West Xianning Road, Xi'an, 710049, P. R. China, E-mail: jianlin@xjtu.edu.cn.

[b] Key Laboratory of Interfacial Physics and Technology, Shanghai Institute of Applied Physics, Chinese Academy of Sciences, 2019 Jia Luo Road, Shanghai 201800, P. R. China, E-mail: wangjianqiang@sinap.ac.cn.

[c] University of Chinese Academy of Sciences, No.19(A) Yuquan Road, Shijingshan District, Beijing, 100049, P. R. China.

[d] State Key Laboratory of Radiation Medicine and Protection, Soochow University, Suzhou, 215123, China

Table of Content

S1. Experimental Section 3

S1.1 Materials and Synthesis 3

S1.2 Characterizations 3

S2. Supplementary Figures and Tables 5

Fig. S1. The coordination environments of Th(2) and Th(4). Color code: Th in cyan, μ_3-OH^-/O^{2-} in red, H_2O in dark blue, O from tpc^- in purple, O from pba^- in pink, O from CH_3COO^- in green, and C in gray. 5

Fig. S2. PXRD pattern of as-synthesized Th-105 compared with the simulated one. 5

Fig. S3. Photoluminescence spectra of Hpba and Htpc under 325 nm UV excitation. 6

Fig. S4. CIE evolution of Th-105 under 365 nm UV and X-ray irradiation. 6

Fig. S5. The ratio between the excimer and monomer emission (I_G/I_B) of Th-105 as a function of UV dose. 7

Fig. S6. The ratio between the excimer and monomer emission (I_G/I_B) of Th-105 as a function of X-ray dose. 7

Fig. S7. Electron paramagnetic resonance spectra of Htpc before and after UV irradiation. 8

Fig. S8. Electron paramagnetic resonance spectra of Hpba before and after UV irradiation. 8

Fig. S9. The FTIR spectra of Th-105 before radiation, after 6h UV radiation, 1 MGy γ-ray or 3 MGy EB radiation. 9

Table S1. Crystallographic data for Th-105. 10

Table S2. The CIE chromaticity coordinates (x, y) of the luminescence of Th-105 in response to increasing dose of UV or X-ray radiation. 11

S1. Experimental Section

S1.1 Materials and Synthesis

Caution! *Th-232 used in this study is an emitter with the daughter of radioactive Ra-228. All of the thorium compounds used and investigated were operated in an authorized laboratory designed for actinide element studies. Standard protections for radioactive materials should be followed.*

Materials. $Th(NO_3)_4·6H_2O$ (99.9%, Changchun Institute of Applied Chemistry, Chinese Academy of Sciences), 3-(pyridin-4-yl)benzoic acid (Hpba), (95%, Jilin Chinese Academy of Sciences - Yanshen Technology Co., Ltd), 2,2':6',2"-terpyridine-4'-carboxylic acid (Htpc) (99%, Jilin Chinese Academy of Sciences - Yanshen Technology Co., Ltd), CH_3COOH (AR, ≥99.5%, Sinopharm Chemistry Reagent Co., Ltd), and dimethylformamide (99.5%, Aladdin), were used as received from commercial suppliers without further purification.

Synthesis. A mixture of $Th(NO_3)_4·6H_2O$ (5.88 mg, 0.01 mmol), 3-(pyridin-4-yl)benzoic acid (Hpba) (2 mg, 0.01 mmol), 2,2':6',2"-terpyridine-4'-carboxylic acid (Htpc) (2.77 mg, 0.01 mmol), CH_3COOH (50 μL), DMF (200 μL), and deionized water (800 μL) were loaded into a 5 mL glass vial. The vial was sealed and heated to 100°C for 72 h and then cooled to room temperature under ambient conditions. Colorless block single crystals of **Th-105** were isolated. The crystals were washed with ethanol and dried under ambient conditions.

S1.2 Characterizations

Crystallographic Analysis. Single crystal X-ray diffraction measurement was performed using a Bruker D8-Venture single crystal X-ray diffractometer equipped with an IμS 3.0 microfocus X-ray source (Mo–Kα radiation, λ = 0.71073Å) and a CMOS detector at 298 K. The data frames were collected using the program APEX3 and processed using the program SAINT routine in APEX3. The structure was solved by Intrinsic Phasing with *ShelXT* and refined with ShelXL using *OLEX2*.

Powder X-ray diffraction (PXRD). PXRD data were collected from 5 to 50° with a step of 0.02° and the time for data collection was 0.2~0.5 s on a Bruker D8 Advance diffractometer with Cu Kα radiation (λ = 1.54056 Å) and a Lynxeye one-dimensional detector.

Photoluminescence Spectroscopy. The solid-state photoluminescence spectra were collected on an Edinburgh Instruments FS-5 steady state spectrofluorometer from a tablet of **Th-105** with 325 nm UV excitation. The decay curves were collected on an Edinburgh Instruments FLS 980 spectrometer from bulk samples. The photoluminescence quantum-yields (PLQYs) were recorded using a HORIBA scientific Fluorolog-3 spectrophotometer with a quantum-yield accessory. The UV radiation was provided by a China Education Au-light Technology CEL-PCRS25 photochemical reactor (365 nm, 25 W, 80 mW cm^{-2} s^{-1}). The X-ray radiation was provided by a W Kα radiation source (60 kV, 12W, 29.79 Gy min^{-1}).

Fourier Transform Infrared (FTIR) Spectroscopy. The FTIR spectra were recorded using a FTIR spectrometer (Thermo Nicolet 6700 spectrometer) equipped with a diamond attenuated total reflectance (ATR) accessory in the range of 400–4000 cm^{-1} .

Electron Paramagnetic Resonance (EPR) Study. The EPR spectra for nonirradiated and irradiated samples was recorded on a JEOL-FA200 spectrometer. An X-band spectrometer (JES-FA200) with 100-kHz field modulation was interfaced with a computer to manipulate the spectra and integrate spectral intensity EPR measurements were performed at room temperature and the microwave power used was 1.0 mW.

Radiolytic Stability. The radiation resistance of **Th-105** were examined by irradiating the powdery sample with UV, electron beam (EB), or γ-ray under ambient conditions. UV, EB and γ-ray radiations were provided by a photochemical reactor (365nm, 25W, 80 mW cm^{-2} s^{-1}), a custom-built electron cyclotron (1.2 MeV, 150 kGy h^{-1}), and a ^{60}Co irradiation source (2.22×10^{15} Bq, 11.8 kGy h^{-1}), respectively. PXRD study on the irradiated samples were performed to evaluate the radiation resistance of **Th-105**.

S2. Supplementary Figures and Tables

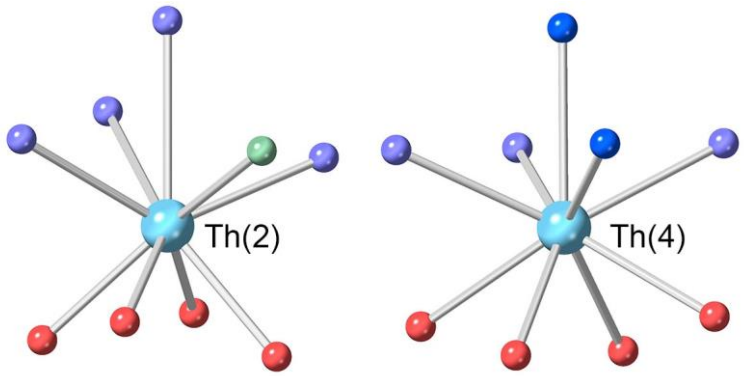

Fig. S1. The coordination environments of Th(2) and Th(4). Color code: Th in cyan, μ_3-OH^-/O^{2-} in red, H_2O in dark blue, O from tpc^- in purple, O from pba^- in pink, O from CH_3COO^- in green, and C in gray.

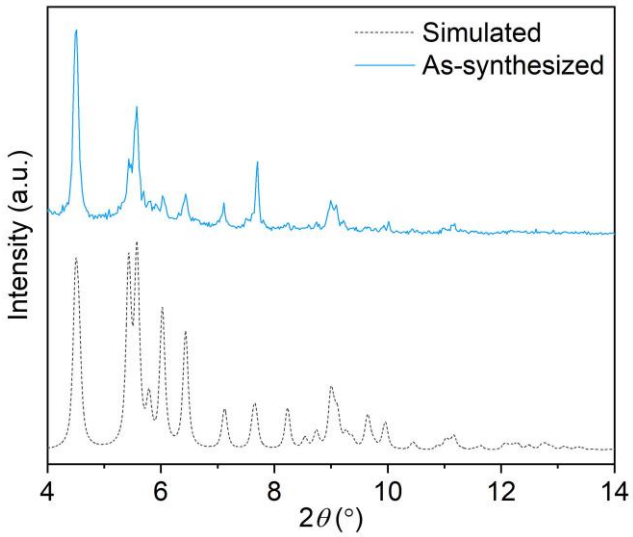

Fig. S2. PXRD pattern of as-synthesized **Th-105** compared with the simulated one.

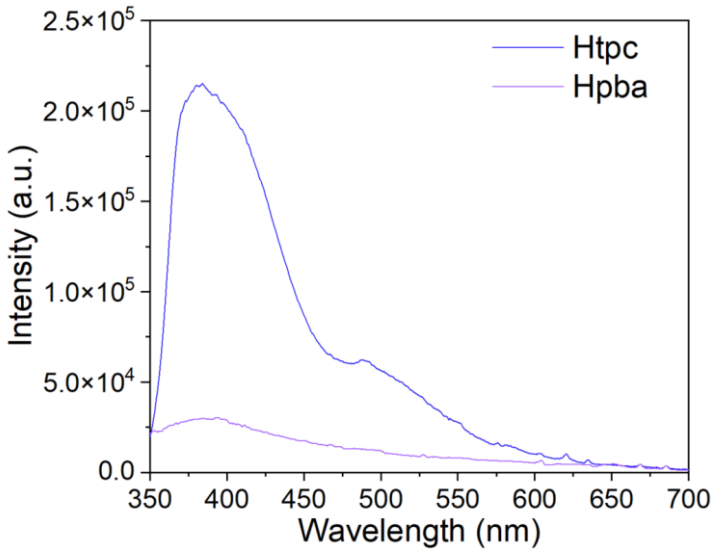

Fig. S3. Photoluminescence spectra of Hpba and Htpc under 325 nm UV excitation.

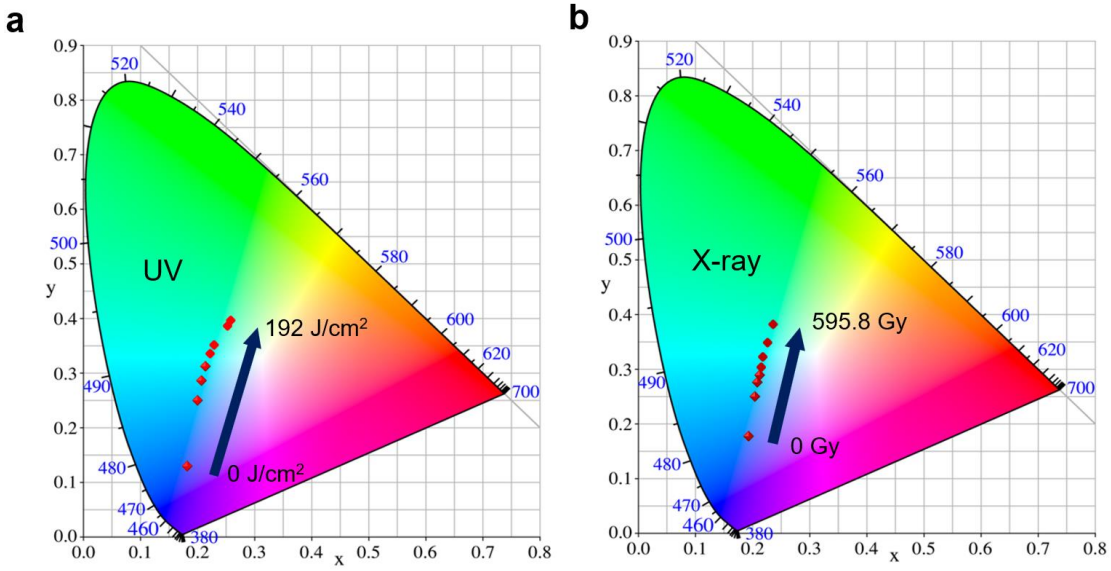

Fig. S4. CIE evolution of **Th-105** under 365 nm UV and X-ray irradiation.

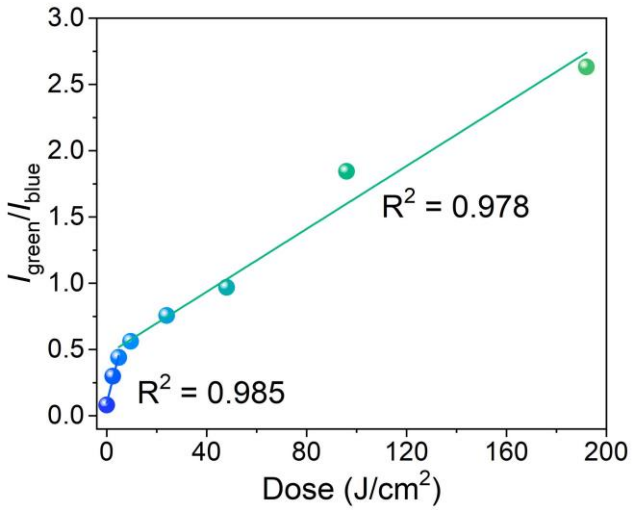

Fig. S5. The ratio between the excimer and monomer emission (I_G/I_B) of **Th-105** as a function of UV dose.

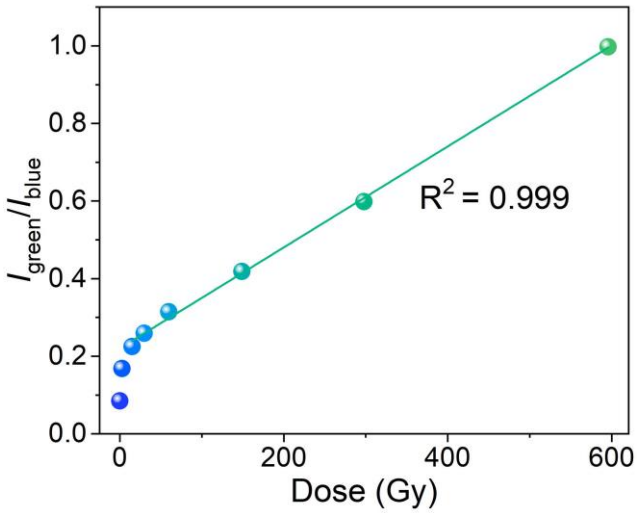

Fig. S6. The ratio between the excimer and monomer emission (I_G/I_B) of **Th-105** as a function of X-ray dose.

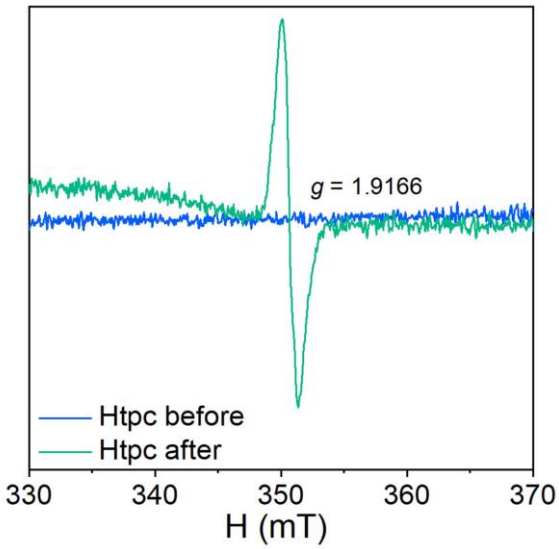

Fig. S7. Electron paramagnetic resonance spectra of Htpc before and after UV irradiation.

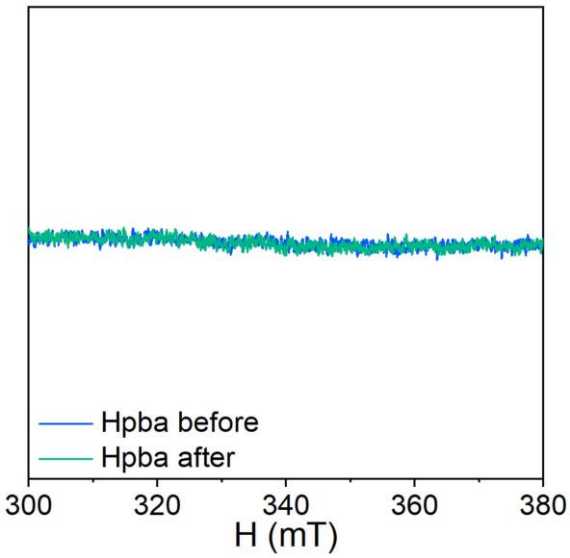

Fig. S8. Electron paramagnetic resonance spectra of Hpba before and after UV irradiation.

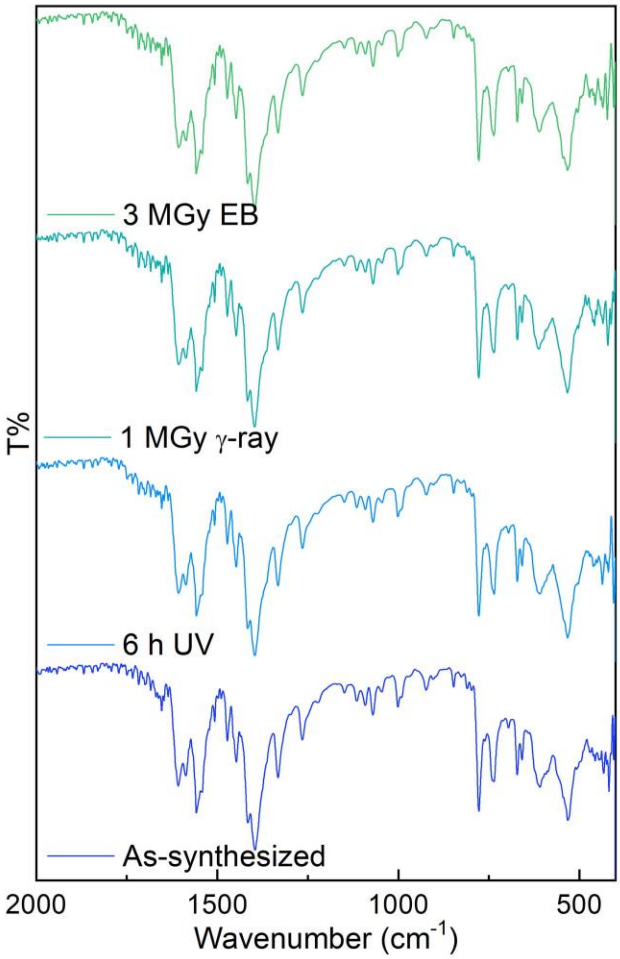

Fig. S9. The FTIR spectra of **Th-105** before radiation, after 6h UV radiation, 1 MGy γ-ray or 3 MGy EB radiation.

Table S1. Crystallographic data for **Th-105**.

Compound	**Th-105**
Mass	4851.43
Color	colorless
Habit	block
Space group	$P\bar{1}$
a (Å)	20.2226(2)
b (Å)	20.2049(2)
c (Å)	23.3410(3)
α (deg)	80.4910(9)
β (deg)	89.9651(9)
γ (deg)	76.2585(9)
V (Å^3)	9145.58(17)
Z	2
T (K)	273
λ (Å)	0.71073
Max 2θ (deg)	50
ρ_{calcd} (g cm^{-3})	1.762
μ (Mo Ka)	0.71073
R_1	0.0376
wR_2	0.0921
Rint	0.0697
GOF	1.150

Table S2. The CIE chromaticity coordinates (x, y) of the luminescence of **Th-105** in response to increasing dose of UV or X-ray radiation.

UV		X-ray	
(J/cm^2)	(x, y)	(Gy)	(x, y)
0	(0.183, 0.129)	0	(0.194, 0.176)
2.4	(0.200, 0.249)	2.48	(0.204, 0.249)
4.8	(0.207, 0.285)	14.9	(0.209, 0.275)
9.6	(0.214, 0.312)	29.79	(0.212, 0.289)
24	(0.223, 0.335)	59.58	(0.215, 0.302)
48	(0.229, 0.351)	148.95	(0.219, 0.322)
96	(0.252, 0.386)	297.9	(0.226, 0.347)
192	(0.258, 0.296)	595.8	(0.236, 0.381)